

Onset of runaway nucleation in aerosol reactors

Jin Jwang Wu and Richard C. Flagan

Division of Engineering and Applied Science, California Institute of Technology, Pasadena, California 91125

(Received 9 January 1986; accepted for publication 28 October 1986)

The onset of homogeneous nucleation of new particles from the products of gas phase chemical reactions was explored using an aerosol reactor in which seed particles of silicon were grown by silane pyrolysis. The transition from seed growth by cluster deposition to catastrophic nucleation was extremely abrupt, with as little as a 17% change in the reactant concentration leading to an increase in the concentration of measurable particles of four orders of magnitude. From the structure of the particles grown near this transition, it is apparent that much of the growth occurs by the accumulation of clusters on the growing seed particles. The time scale for cluster diffusion indicates, however, that the clusters responsible for growth must be much smaller than the apparent fine structure of the product particles.

I. INTRODUCTION

When gas phase chemical reactions generate low vapor pressure species in excess of their equilibrium vapor pressure, the vapors may deposit on existing surfaces or, if large excess of condensable species is produced, the vapors may form new particles by homogeneous nucleation. New particle formation may be desirable if the reactions are being carried out to produce a powder, such as in the synthesis of fine powders for ceramics application; however, it is frequently desirable to prevent homogeneous nucleation. In the production of submicron particles for use in the synthesis of ceramics or other bulk structures, the high number concentrations produced by uncontrolled nucleation lead to the formation of undesirable agglomerates by Brownian coagulation. Powders comprised of agglomerates, therefore, present problems in subsequent processing.¹ The feasibility of suppressing nucleation of refractory vapors has recently been demonstrated by growing small seed particles of Si to sizes in excess of $10\ \mu\text{m}$ by silane pyrolysis in an aerosol reactor.²

Control of homogeneous nucleation is, thus, central to a number of technologies involving vapor deposition. In this paper, we examine the onset of homogeneous nucleation in reacting systems, using seed particles to probe the factors that limit new particle formation. The range of reactor operating conditions in which the formation of stable new particles can be completely suppressed is mapped. The enhanced growth of silicon particles above micron size by scavenging of the products of gas phase reactions has been proven effectively. The structure of the particles grown in the reactor provides insight into the mechanisms of particle formation and growth as well as into chemical vapor deposition.

II. EXPERIMENTAL SYSTEM

The reactor system used in this study was extended from a system developed for the growth of large silicon particles by silane pyrolysis.² The present three stage reactor is illustrated in Fig. 1. Seed particles were produced by pyrolyzing a small amount of silane (1% by volume in atmospheric pressure nitrogen) in a 10-mm i.d., 125-mm-long stainless-steel tube that was heated to 1100 K. The residence time in

this reactor was long, about 25 s, so appreciable coagulation of the nuclei occurred. The particle size at the outlet to this reactor stage ranged from 0.1 to $0.3\ \mu\text{m}$ as measured with a TSI model 3070 electrical aerosol size analyzer.

To extend the range of seed particle sizes for the present study, a seed growth reactor was added to the original two-stage system. The aerosol was cooled at the outlet of the first reactor stage and mixed with dilute silane (1% by volume). A series of static mixers was used to ensure thorough mixing of the seed particles with the reactant, since, if composition inhomogeneities were allowed to persist, runaway nucleation in particle-free regions of the flow would dramatically increase the mean particle number concentration and interfere with the interpretation of our experimental results. The seed growth reactor (stage 2 in Fig. 1) consisted of a 10-mm i.d., 350-mm-long quartz tube that was heated in four zones of 50 mm length. These zones were separated by 10-mm-thick insulation so that smoothly varying wall temperature profiles could be achieved. The midpoint reactor wall tem-

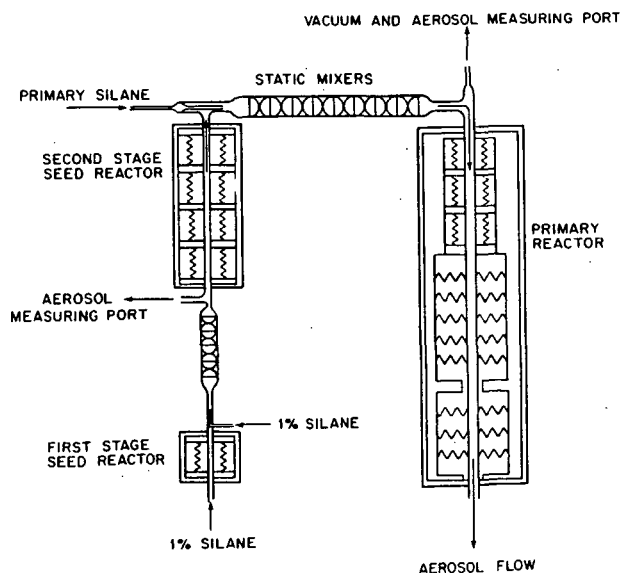


FIG. 1. Schematic of the three-stage aerosol reactor.

peratures of the four zones were 680, 780, 840, and 1100 K. Ramping the temperature in this way gradually accelerates the decomposition of silane as the seed particles grow and become more effective at suppressing nucleation.² With this two-stage seed generation system, seed particles ranging from 0.2 to 2.0 μ in diameter were generated with number concentrations ranging from 10^4 to 10^6 cm^{-3} .

Our primary concern was the onset of nucleation in the final growth reactor, stage 3 in Fig. 1. The seed particles leaving the second stage were mixed with additional silane and nitrogen, again using a series of static mixers, before entering this reactor stage. The primary reactor was an 850-mm-long quartz tube with an internal diameter of 12 mm. It was heated in five separate zones: three 50-mm-long zones similar to those of stage 2, followed by 300- and 150-mm-long zones that were heated with Lindbar silicon carbide heating elements. The zones were again separated by insulating layers to facilitate the establishment of a smooth temperature profile along the length of the reactor. The measured temperature profiles on the growth reactor wall are shown in Fig. 2, and the heating zones are indicated. The temperatures in the first four stages of the reactor were kept constant for all of the experiments reported here. This profile was selected since particles could be grown, without significant increase in the number concentration, with a seed aerosol consisting of 10^5 cm^{-3} of 0.7- μm particles, and 1% silane. For these conditions, silane pyrolysis was completed within the fourth heating zone. The temperature in the final heating zone was varied as shown in Fig. 2 in order to alter the structure of the enlarged silicon particles as described below.

The silicon aerosol was characterized using a battery of particle sizing and counting instruments: (1) a Royco model 226 laser optical particle counter with resolution in the 0.12 to 6 μm size range; (2) a particle measurement systems classical scattering optical particle counter (0.5–47 μm); and (3) a Rich 100 environment one condensation nucleus counter (total number concentration of particles larger than about 20 nm). The latter instrument was calibrated using a

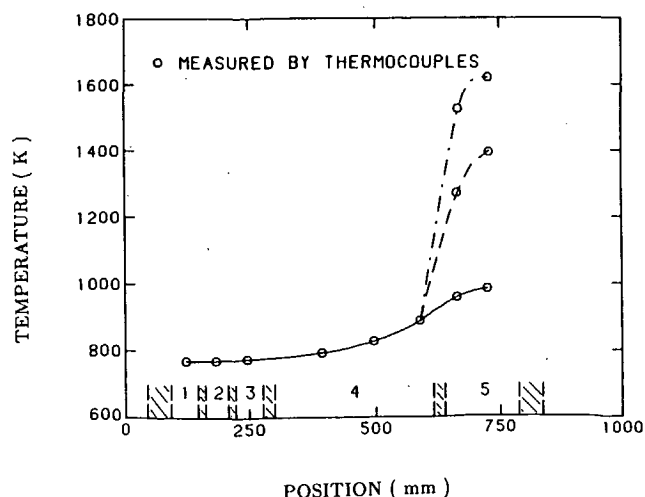


FIG. 2. Measured temperature profiles on the primary reactor wall. The heating zones and regions of insulation are indicated.

TSI model 3030 differential mobility classifier with the Faraday cup/electrometer assembly from a TSI model 3070 electrical aerosol size analyzer used as a detector.

The aerosol leaving the growth reactor was diluted with nitrogen as illustrated in Fig. 3, to ensure compatibility with these instruments, which were designed for the characterization of aerosols at the much lower concentrations found in the atmosphere. The first dilution stage served the dual purposes of reducing the concentration of particles and minimizing the thermophoretic losses of particles on the cold wall as the hot aerosol was cooled. This was accomplished by transpiring the nitrogen diluent through the wall of a sintered stainless-steel tube. In the second stage diluter, some of the reaction products are filtered and then recirculated to dilute the aerosol 200:1 to 2000:1 with a minimum of uncertainty concerning the dilution ratio.

Aerosol samples were also collected using Teflon filters for study by x-ray diffraction, scanning electron microscopy, and gas adsorption.

III. EXPERIMENTAL RESULTS AND DISCUSSIONS

To use the changes in the silicon aerosol in the growth reactor to explore the nucleation process, it was first necessary to verify that no changes occurred within this reactor stage in the absence of chemical reactions. Figure 4 shows the size distribution of the seed aerosol produced by reaction of 35 cm^3 min^{-1} (STP) of 1% silane as measured (1) after dilution with nitrogen at the outlet of the seed generator, Stage 2, (2) at the entrance to the growth reactor, and (3) at the outlet of the growth reactor. As the aerosol passed through the static mixers, only about 10% of the mass was lost to the walls, but the number concentration decreased markedly due to coagulation and diffusion of small particles to the surfaces. The change in the growth reactor was much less pronounced, although there again was a slight shift to larger particle sizes due to coagulation. The close correspondence of the concentrations at the inlet and outlet of the growth reactor demonstrates the efficacy of the transpired

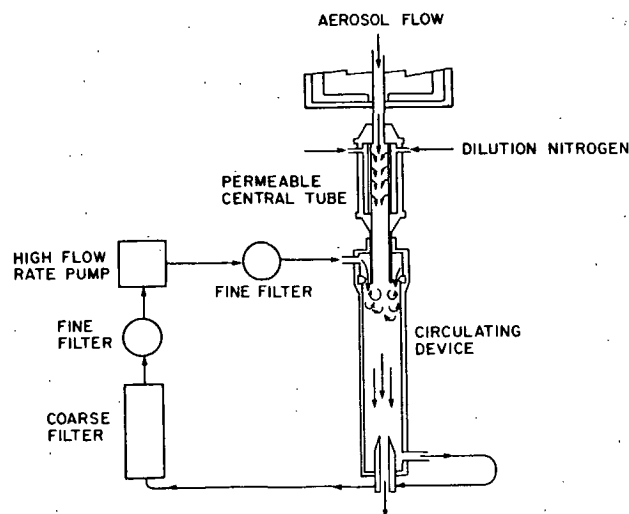


FIG. 3. Schematic of the aerosol dilution system showing the transpired wall first stage and recirculating second stage.

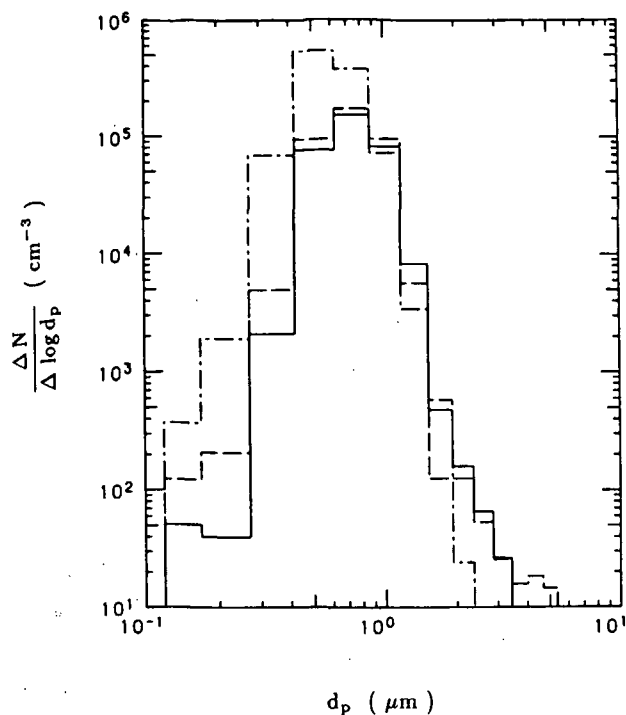


FIG. 4. Size distributions of the seed aerosol produced by reaction of $35 \text{ cm}^3 \text{ min}^{-1}$ (STP) of 1% silane as measured: (dash-dot-dash) after dilution with nitrogen at the outlet of the seed generator, stage 2; (dashed) at the entrance of the growth reactor; and (solid) at the outlet of the growth reactor.

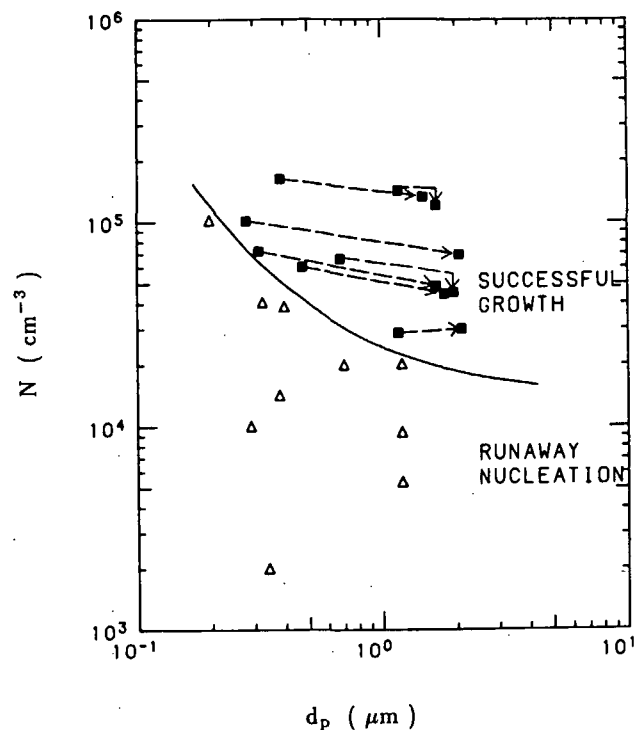


FIG. 5. Map of reactor operating conditions leading to successful growth of seed particles (solid points connecting initial and final conditions) and catastrophic nucleation (open points indicating initial conditions). The reactor temperature profile corresponds to the solid curve in Fig. 2. The reactant gas consisted of 1% silane in nitrogen.

wall diluter in preventing thermophoretic deposition. In previous experiments conducted without this device, as much as 99% of the particles was deposited on the wall in the cooling region. Thus, changes in the aerosol in the seed generator were small when no reaction occurred, and the changes observed in the reaction experiments can be attributed directly to the effects of the silane decomposition reactions.

The growth of small seed particles to sizes in excess of a micron has previously been demonstrated in a two-stage version of this reactor.² In the present study, the transition from particle growth by cluster deposition to catastrophic nucleation was explored by varying the seed aerosol characteristics for a reactor flow rate, silane concentration, and temperature profile for which growth without nucleation had been achieved. The temperature profile was the solid curve in Fig. 2, with a flow of $600 \text{ cm}^3 \text{ min}^{-1}$ of 1% silane in nitrogen. Two modes of reactor operation were observed as the seed particle size and number concentration were varied: (1) growth of the seed particles at approximately constant number concentration; and (2) nucleation producing very large numbers of very small particles leading to a large increase in the number concentration and a corresponding decrease in the mean particle size. The former results are plotted in Fig. 5 as pairs of solid points connecting the initial and final mean particle sizes and number concentrations. The latter results are indicated as open points showing only the initial seed aerosol properties. The total mass of the product was measured using filters to determine the efficiency of conversion of silane to silicon powder. About 80% of silicon was recovered when 1% silane was reacted. Similar results were ob-

tained in previous experiments in the two-stage reactor.² It was determined experimentally that, for 1% silane in the feed gas, about one third of the total loss occurred in the dilution system.

The transition between these two operating domains was extremely abrupt, depending on both the size and the number concentration of the seed particles. This transition can be seen more clearly by examining the effect of changing the reactant silane concentration on the final number concentration for otherwise constant reactor operation and seed aerosol characteristics, as illustrated in Fig. 6. In these experiments, a seed aerosol of 10^5 cm^{-3} $0.7\text{-}\mu\text{m}$ particles was reacted with silane mole fractions up to 5%. The temperature profile used was the same as for Fig. 5. The seed aerosol is indicated as the point for 0% silane. The total number concentration as measured by the condensation nucleus counter (CNC) increased by about 50% as the silane mole fraction was increased to 3%. Further increasing to 3.5% silane resulted in an increase in the number concentration of four orders of magnitude. Increasing the silane concentration beyond that value did not appreciably alter the number concentration of the product aerosol, presumably due to the coagulation of the fine particle produced by homogeneous nucleation. As noted, the CNC measured slightly higher number concentrations than the optical particle counters due to the smaller size detection limit of the former instrument.

The physical structure of the particles grown at silane concentrations below that which leads to runaway nucleation provides additional insights into the nucleation process.

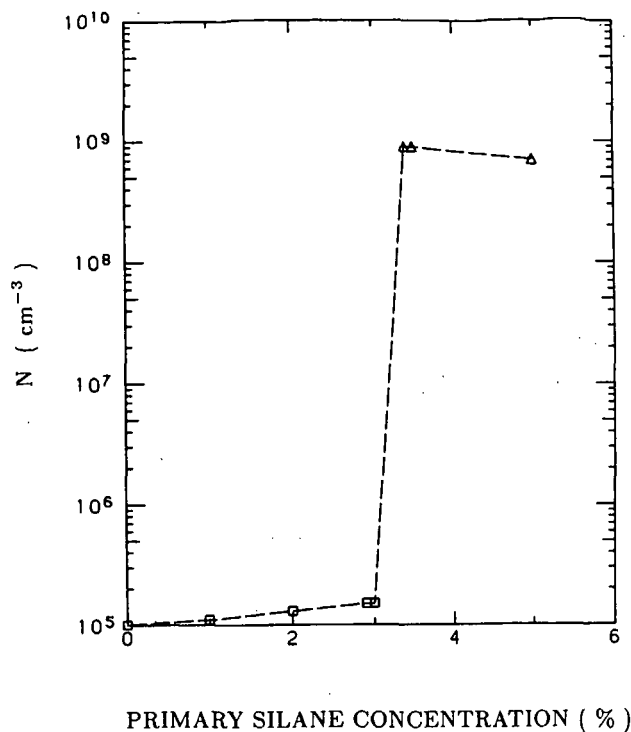


FIG. 6. The influence of silane concentration on the final number concentration for fixed temperature profile (the solid curve in Fig. 2) and seed aerosol [10^5 cm^{-3} (STP) seed particles of $0.7 \mu\text{m}$ diameter].

Figure 7 shows a typical seed particle. It is clearly not a dense spherical particle, since the seed reactor temperature was not high enough to densify particles of this size. Figure 8 shows a particle that has been grown in the primary reactor. It too appears to be the result of particle growth by coagulation, consisting of an assemblage of small spheres of approxi-

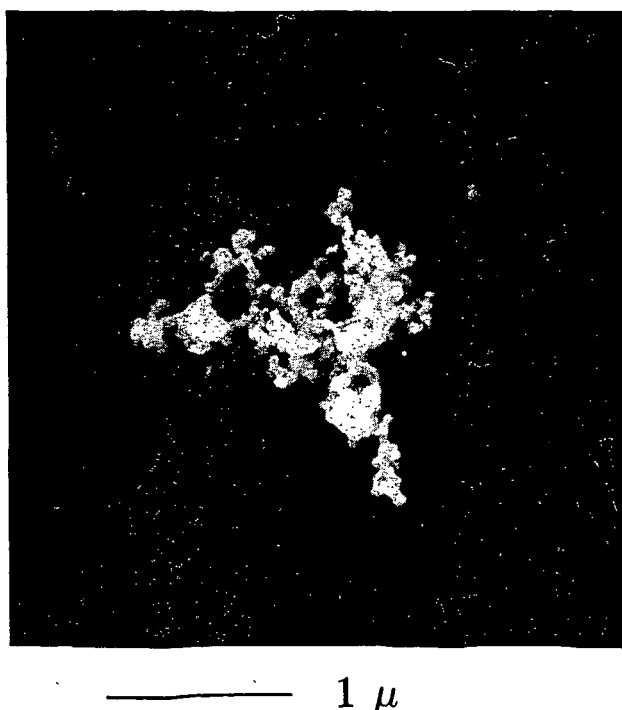
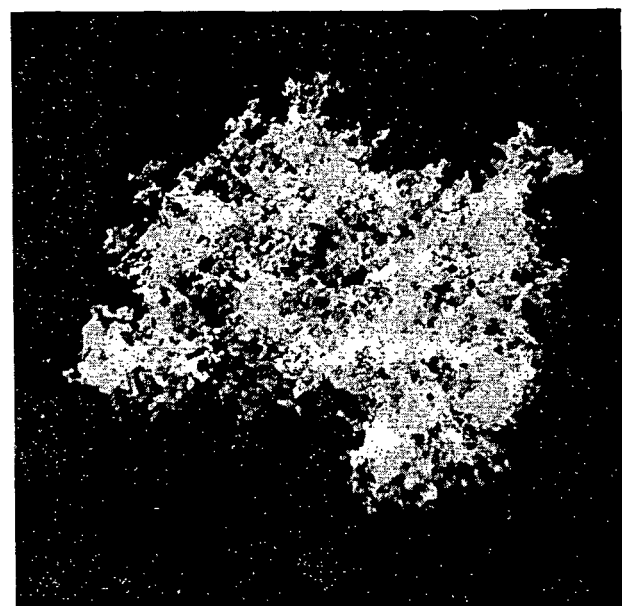


FIG. 7. SEM micrograph of a seed particle.



— 0.1 μ



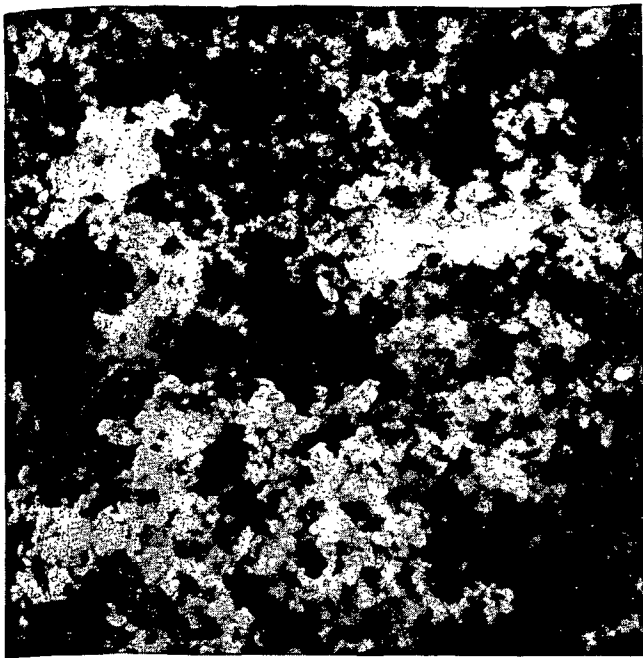
— 10 μ

FIG. 8. SEM micrograph of the product particle generated with a maximum reactor temperature of 973 K.

mately $0.1 \mu\text{m}$ in diameter. The apparent surface area measured by nitrogen adsorption and interpreted using the BET isotherm³ was $20.3 \text{ m}^2 \text{ g}^{-1}$. The helium displacement density was 2.3 g cm^{-3} , corresponding to a mean sphere size of $0.13 \mu\text{m}$. These indicate that this agglomerate structure is uniform throughout the particle volume.

As we shall demonstrate later, the diffusivities of $0.1\text{-}\mu\text{m}$ particles are, however, so low that the observed growth of the seed particles and the small increase in the number concentration cannot be attributed to the coagulation of these particles with the seeds. Instead, the structure of the particles must be the result of partial sintering of low density particles which initially had a much finer structure. To verify this assumption, the particles shown in Fig. 9 were grown with a peak temperature of 773 K. As one would expect if surface or bulk diffusion were responsible for the coalescence, the particles grown at this low temperature have a structure that is even finer than that of the particle in Fig. 8.

For further support for this assumption and for proof



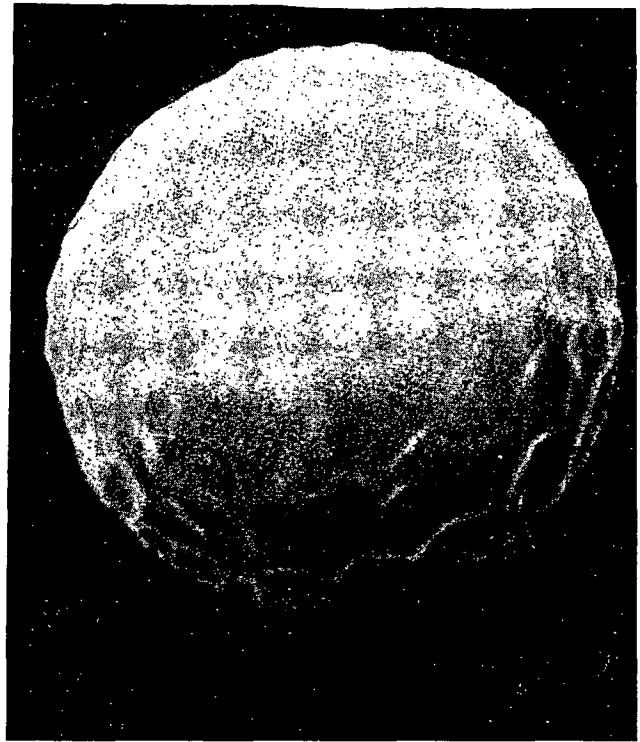
— 1 μ

FIG. 9. Close view of the product particle generated with a peak temperature of 773 K.

that the agglomerate structure is not an artifact of the sample collection process, the temperature in the final zone of the primary reactor was raised to higher values for sintering the suspended particles to a fully dense state. The reactor was designed so that this could be done without significantly altering the temperature profile in the upstream regions where the silane decomposition and particle growth took place. Figure 10 shows the densified particles that resulted when the final zone temperature was increased to 1723 K. The residence time in this final heating zone was approximately 1 s, so the changes shown occurred in a relatively short time.

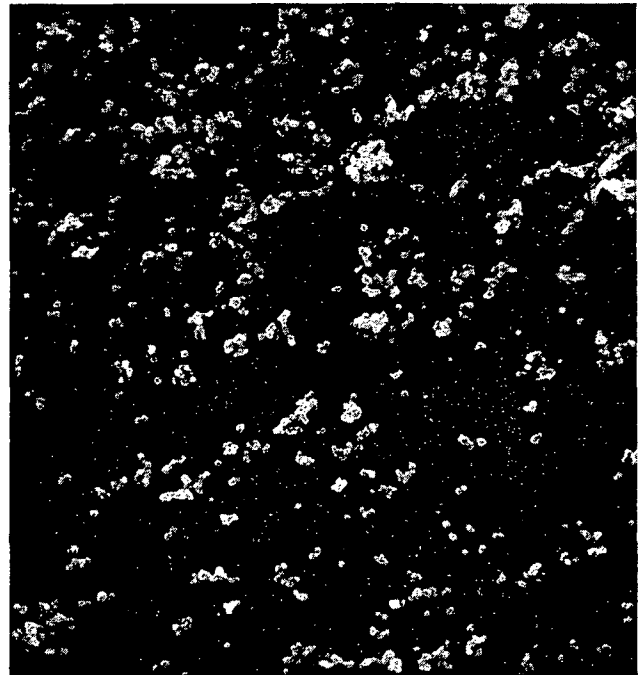
Figure 11 is a micrograph of the particles that resulted from catastrophic nucleation when 3.5% silane was reacted using the temperature profile indicated by the solid curve in Fig. 2. The sizes of these particles appear to be on the same order as the fine structure of the successfully grown particles at the same temperature (Fig. 8). This indicates the sintering effect. By assuming that the nucleated particles would finally grow to $0.1 \mu\text{m}$ with bulk silicon density, the number concentration from successful particle growth to runaway nucleation in Fig. 6 should change from 10^5 to $2.8 \times 10^9 \text{ cm}^{-3}$ based on a mass conservation calculation. The calculated number concentration due to runaway nucleation is a little higher than observed. The lower concentration could result from deposition of some condensable vapors on the seeds, appreciable coagulation between particles at these higher number concentration, and loss in the system.

The x-ray diffraction patterns of particles that have undergone different post-thermal treatment due to the increase in the temperature of the final zone are shown in Fig. 12. The powders processed at lower temperatures than 973 K were



— 1 μ

FIG. 10. SEM micrograph of product particle following post-growth processing at elevated temperature (1723 K) for approximately 1 s.



— 2 μ

FIG. 11. SEM micrograph of the particles that resulted from catastrophic nucleation.

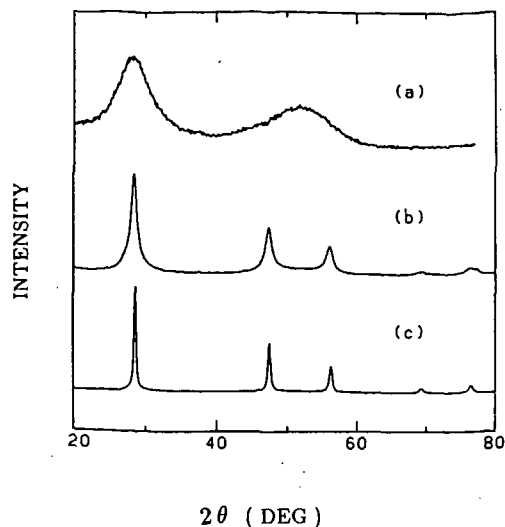


FIG. 12. X-ray diffraction patterns of particles that have undergone different post-thermal treatment due to the increase in the final zone temperature.

clearly amorphous. As the treatment temperature was increased, the material gradually shifted from an amorphous to a more ordered crystalline structure.

A simple calculation shows that the particles could not have grown as observed, without an increase in the number concentration, by coagulation of particles of $0.1 \mu\text{m}$ diameter. Figure 13 shows the characteristic time τ for loss of clusters of size $d_{p,c}$ with the density of bulk silicon by Brownian coagulation with seed particles of various sizes $d_{p,s}$, also

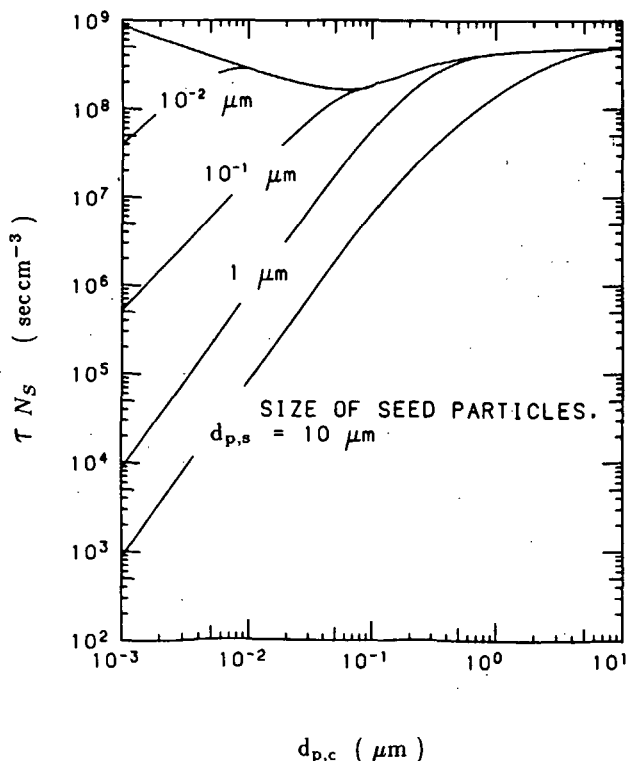


FIG. 13. Characteristic time for loss of clusters of size $d_{p,c}$ by Brownian coagulation with seed particles of various sizes $d_{p,s}$ and number concentration N_s .

assumed to be dense spheres. These times are defined as $1/N_s \beta(d_{p,s}, d_{p,c})$, where N_s is the number concentration of seed particles and $\beta(d_{p,s}, d_{p,c})$ is the Brownian coagulation coefficient. Fuchs' interpolation formula⁴ with Millikan's slip correction for the particle diffusivity⁵ was used for particles ranging from the free molecule ($K_n = 2\lambda/d_p \gg 1$) to the continuum ($K_n \ll 1$) size range.⁶ The enhancement of coagulation between the particles by intermolecular forces was found to be negligible. Typical seed aerosols in our experiments contained 10^5 to 10^7 cm^{-3} particles of order $1 \mu\text{m}$ in size. If $0.1\text{-}\mu\text{m}$ particles were produced, the time for their loss by coagulation with the seeds would be on the order of 10–1000 s, much longer than the 1–10 s, during which the aerosol remains in the reactor. Only particles on the order of $0.01 \mu\text{m}$ in diameter, or smaller, would be efficiently scavenged by the seed particles within this short time. The assumption that the particles are dense spheres is clearly an oversimplification since, as we have seen, the particles grown at low temperatures in the aerosol reactor have relatively low densities and considerable fine structure. This does not, however, significantly alter the time scales for cluster scavenging. In the coagulation of particles of grossly dissimilar size, the motion of the smaller particle dominates. Thus, the projected area of the larger particle is more important than its mobility. The time required for sintering a small cluster of particles to full density is short due to the large surface free energy. The diffusion of dense spheres, such as those shown in Fig. 11, is accurately described by this model. The main deficiency of this model is, therefore, in the estimation of the seed density. For large seed particles, $\tau \propto d_{p,s}^{-1}$ or $\tau \propto \rho_{p,s}^{1/3}$, and the influence of density of the large particle is relatively weak.

It is believed, therefore, that the seed particles were grown by the deposition of clusters much smaller than $0.1 \mu\text{m}$. As the clusters accumulated, they partially sintered together to form the fine structure of the final aerosol. Since the sintering rate increases with increasing temperature, the size of the fine structures are larger at higher final zone temperature, with the particles becoming more densified. Ultimately, when the final zone temperature is increased to the melting point, dense spherical particles are formed.

IV. CONCLUSION

The transition from particle growth to runaway nucleation is extremely abrupt. The structure of the particles grown near this transition suggests that the diffusion of small clusters accounts for much of the growth. Gas phase reactions produce very large numbers of clusters that then grow by coagulation and vapor deposition and may be lost by coagulation with the larger seeds. The characteristic times for coagulation indicate that the clusters responsible for the seed particle growth must have been much smaller than the apparent fine structure of the product particles. The abrupt transition from successful seed growth to catastrophic nucleation may be explained in terms of these very small clusters. Since the diffusivity decreases rapidly with cluster size, $D \propto d^{-2}$, only very small clusters can be scavenged efficiently by the seed aerosol. Once the clusters grow too large to diffuse to the seeds within the available residence time,

large numbers of clusters survive to compete with the seeds for the condensable reaction products, thereby limiting the seed particle growth and greatly increasing the total number concentration in the product aerosol. The apparent suppression of nucleation in the aerosol reactor is, therefore, an indication that clusters possibly larger than the critical nucleus of classical nucleation theory do not grow past the point where scavenging is effective.

ACKNOWLEDGMENTS

The assistance of B. Ellen Johnson in constructing the aerosol flow reactor system and Patrick F. Koen in performing the scanning electron microscopy is gratefully acknowl-

edged. The research described in this paper was carried out for the Flat-Plat Solar Array Project, Jet Propulsion Laboratory, California Institute of Technology, and was sponsored by the U.S. Department of Energy through an agreement with NASA.

¹H. K. Bowen, *Mater. Sci. Eng.* **44**, 1 (1980).

²M. K. Alam and R. C. Flagan, *Aerosol Sci. Technol.* **5**, 237 (1986).

³P. C. Hiemenz, *Principles of Colloid and Surface Chemistry*, edited by J. J. Lagowski (Dekker, New York, 1973).

⁴N. A. Fuchs, *The Mechanics of Aerosols* (Pergamon, New York, 1964).

⁵R. A. Millikan, *Phys. Rev.* **22**, 1 (1923).

⁶M. Sitarski and J. H. Seinfeld, *J. Colloid Interface Sci.* **61**, 261 (1977).